Electronic Supplementary Material (ESI) for *Dalton Trans*.
This journal is © The Royal Society of Chemistry 2023

Isolation of potassium salt of oxadiazole-2-thione and *In Vitro* Anticancer Activities of its Cu(II) and Zn(II) complexes against MDA-MB-231 human breast carcinoma cells

M.K. Gond[a], Nilesh Rai[b], Brijesh Chandra, Vibhav Gautam[b], Somenath Garai[a], R.J. Butcher[c], M. K. Bharty[a,*]

[a] Department of Chemistry, Banaras Hindu University, Varanasi-221005, India.

E-Mail: manoj_vns2005@yahoo.co.in; mkbharty@bhu.ac.in

[b] Centre of Experimental Medicine and Surgery, Institute of Medical Sciences, Banaras Hindu University, Varanasi 221005, India.

[c] Department of Chemistry, Howard University, 525 College Street NW, Washington, DC 20059, USA

Contents

1. Materials and methods

Commercial reagents were used without further purification and all experiments, if otherwise mentioned, were carried out in an open atmosphere. Isonicotinic acid hydrazide, CS_2 and KOH were used as received. All the solvents were purchased from Merk Chemicals, India, and used after purification. The carbon, hydrogen, and nitrogen contents were estimated on a Carlo Erba 1108 model micro analyzer. Electronic spectra were recorded on a SHIMADZU 1700 UV-Visible spectrophotometer. Infrared spectra were recorded in the 4000-400 cm^{-1} region as KBr pellets on a PerkinElmer Spectrum Version 10.4.3 3100 FT-IR spectrophotometers. ^{1}H and ^{13}C NMR spectra were recorded in DMSO-d_6 on a JEOL AL 300 FT-NMR spectrometer using TMS as an internal reference.

1.1 DNA protective assay

To determine the *in vitro* antioxidant activity of the Kpot·H_2O and its complexes **1** and **2** against Fenton's reagent mediated hydroxyl radicals, DNA damage protective assay was performed [1]. In this assay, pBR322 plasmid DNA (0.5 µg) was mixed with Fenton's reagent (80 mM $FeCl_3$, 30 mM H_2O_2 and 50 mM ascorbic acid) and different concentrations of the ligand and metal complexes (5 µM and 10 µM) in a ratio of 1:1 (v/v). The volume (20 µL) of the reaction mixture was maintained by Milli-Q water and incubated for 15 minutes at 37 ^{o}C. The reaction mixture containing DNA of pBR322 plasmid and Fenton's reagent was taken as the positive control whereas, only DNA of pBR322 plasmid was as the negative control. Post-incubation, the 10 µL of the reaction mixture was subjected to gel electrophoresis onto 1% agarose, and the gel image was taken using a Gel Doc EZ imager (Bio-Rad, USA).

1.2 Cell culture maintenance and evaluation of *in vitro* cytotoxicity

The MDA-MB-231 cells (human breast cancer cell line) was cultured in Dulbecco's Modified Eagle Medium (DMEM), containing fetal bovine serum (10%) and streptomycin/penicillin solution (1%) [2]. The cell culture was maintained in a CO_2-incubator at 37 °C with 5% CO_2 and humidity. Routine observations were made to assess the proliferation of adherent cells forming a monolayer with 80-90% confluence, while ensuring that there was no contamination. The cytotoxic potential of Kpot·H_2O and its complexes **1** and **2** against MDA-MB-231 cells were evaluated using the 3-(4,5-dimethylthiazol-2-yl)-2,5-diphenyl-2H-tetrazolium bromide (MTT) assay with minor modifications, as previously described [3]. This assay is a crucial step performed on any chemical entity to determine its potential as a drug. In a 96-well plate, a total of 5 x 10^3 MDA-MB-231 cells were seeded and

treated for 24 hours with varying concentrations (5, 25, 50, 75, 100, and 200 µg/mL) of Kpot·H_2O and its complexes **1** and **2**, and tamoxifen (positive control). Thereafter, the media was removed and 150 µL of MTT (SRL) (0.5 mg/mL) was supplemented to each well, followed by a further 4-hours of incubation before being centrifuged for 20 minutes at 3000 rpm. The media containing MTT was then gently taken out, and 100% DMSO (100 µL) was to employed to dissolve the resulting crystals of formazan, and thereafter the absorbance was taken at 570 nm using a microplate reader (Thermo Scientific, USA). The following formula was used to determine the % cell viability:

Cell viability %: [($Abs_{(570nm)}$ of the treated sample / $Abs_{(570nm)}$ of the control)] x 100.

1.3 Analysis of nuclear morphology

In order to assess the effect of Kpot·H2O and its complexes **1** and **2** on the cellular integrity and nuclear morphology of MDA-MB-231, 4',6-diaminodino-2-phenylindole (DAPI) fluorescent dye was employed [4]. A total of 1 x 10^5 MDA-MB-231 cells were seeded onto sterile cover slip placed in a 6-well plate and exposed to the IC_{50} concentrations of Kpot·H_2O and complexes **1** and **2**. Following the treatment for 24 hours, the cells were gently washed with sterile 1X phosphate buffer saline (PBS) and incubated with 70% methanol for 20 minutes at -20°C. Subsequently, the cells were stained at room temperature with DAPI (Puregene, Genetix) for 15 minutes, and images of the DAPI stained cells were taken through fluorescence microscope (Leica, Germany).

1.4 Wound healing assay

To investigate the effect of Kpot·H_2O and its complexes **1** and **2** on the gap-filling ability of MDA-MB-231 cells, wound healing assay was performed [5]. A total of 2 × 10^5 MDA-MB-231 cells were seeded in 6-well plate and allowed to form a uniform monolayer after 24 hours. Subsequently, a constant gap was created by scraping the monolayer using a 20-200 µL pipette tip, followed by gentle rinsing with 1X sterile PBS. Thereafter, cells were treated with Kpot·H_2O and its complexes **1** and **2** for 24 hours, and images were obtained using an inverted microscope (ZEISS Axio Vert A1) at 0 and 24 hours. Using the image analysis software Image J, the length of the cell-free zone was measured, and presented using the equation shown below:

$$\% R = \left[1 - \left(\frac{\text{wound length at } T_{24h}}{\text{wound length at } T_{0\,h}}\right)\right] \text{x } 100$$

Where, % R denotes the percentage of recovery, while T_{0h} and T_{24h} respectively refer to the wound length at 0 hours and 24 hours.

1.5 Caspase-3 activity

To evaluate the activity of Caspase-3 in MDA-MB-231, the Caspase-3 Activity Assay Kit (E-CK-A311A) was used in accordance with the manufacturer's instructions. In brief, 2×10^5 MDA-MB-231 cells were treated with IC_{50} values of Kpot·H_2O and its complexes **1** and **2** for 24 hours when they reached 70-80% confluency. Subsequently, cells were lysed using 2 mM DTT containing lysis buffer, followed by centrifugation to collect the protein-containing supernatant. The supernatant was incubated with the substrate for Caspase-3, Ac-DEVDpNA, in the reaction buffer and incubated for 4 hours at 37 ºC, after which the level of Caspase-3-mediated release of pNA was quantified at 405 nm wavelength by microplate spectrophotometer (Thermo Scientific) [6].

1.6 Statistical analysis

Each experiment was carried out three times independently, and the results were reported as mean ± S.D. To compare between the groups, one-way ANOVA followed by Tukey's test was conducted. Statistical significance was determined using a p-value ***, $p\leq0.001$; **, $p\leq0.002$; *, $p\leq0.033$.

2. IR spectrum Figures

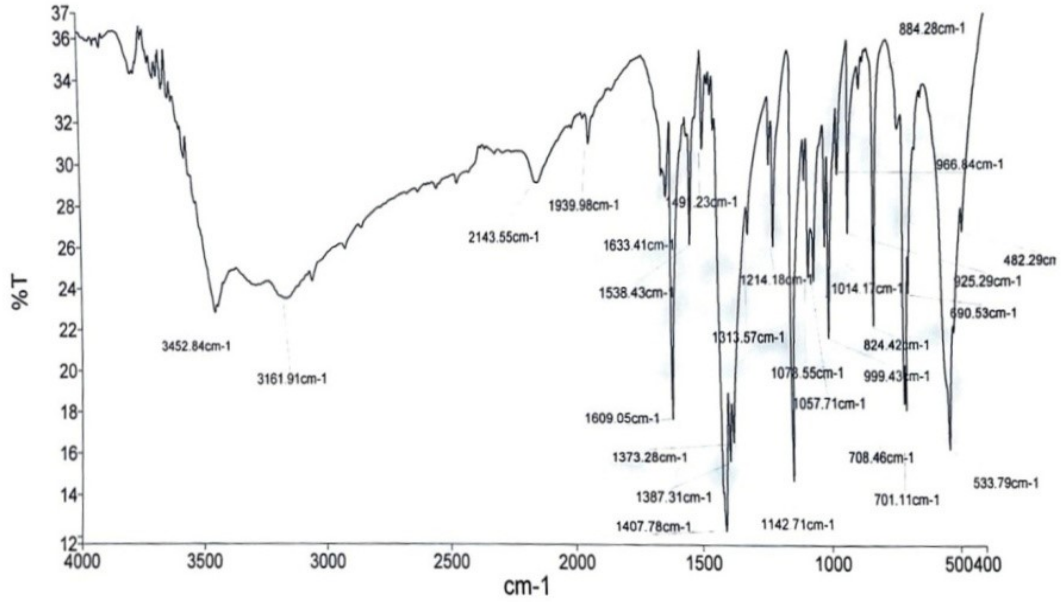

Supplementary Fig. 1. IR spectrum of Kpot·H_2O

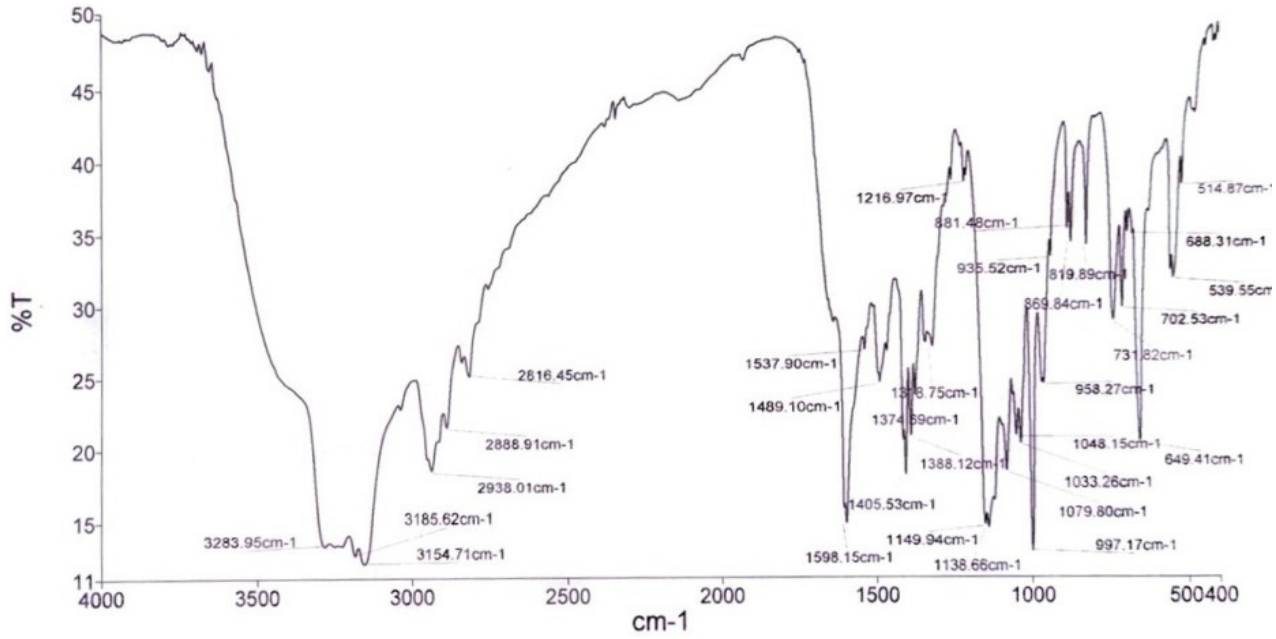

Supplementary Fig. 2. IR spectrum of $[Cu(en)_2](pot)_2]$ (**1**)

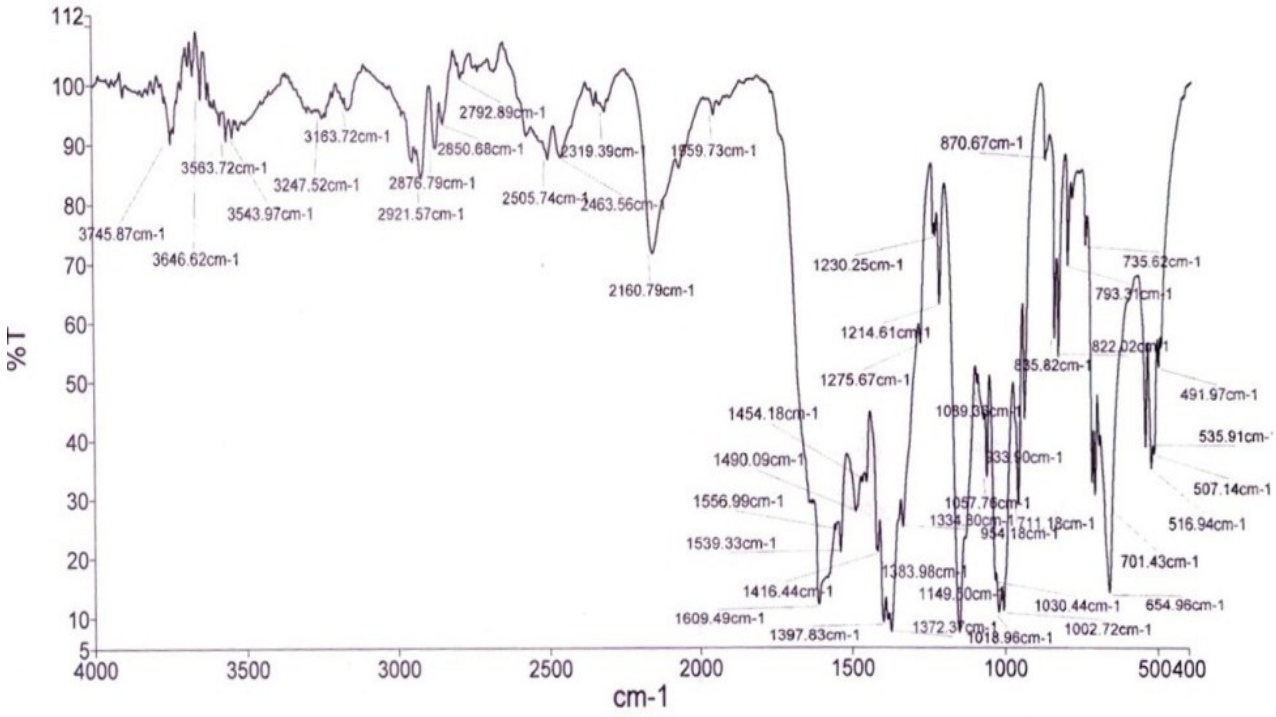

Supplementary Fig. 3. IR spectrum of $[Zn(en)_2(pot)_2HBr \cdot CH_3OH$ (**2**)

3. NMR spectrum Figures

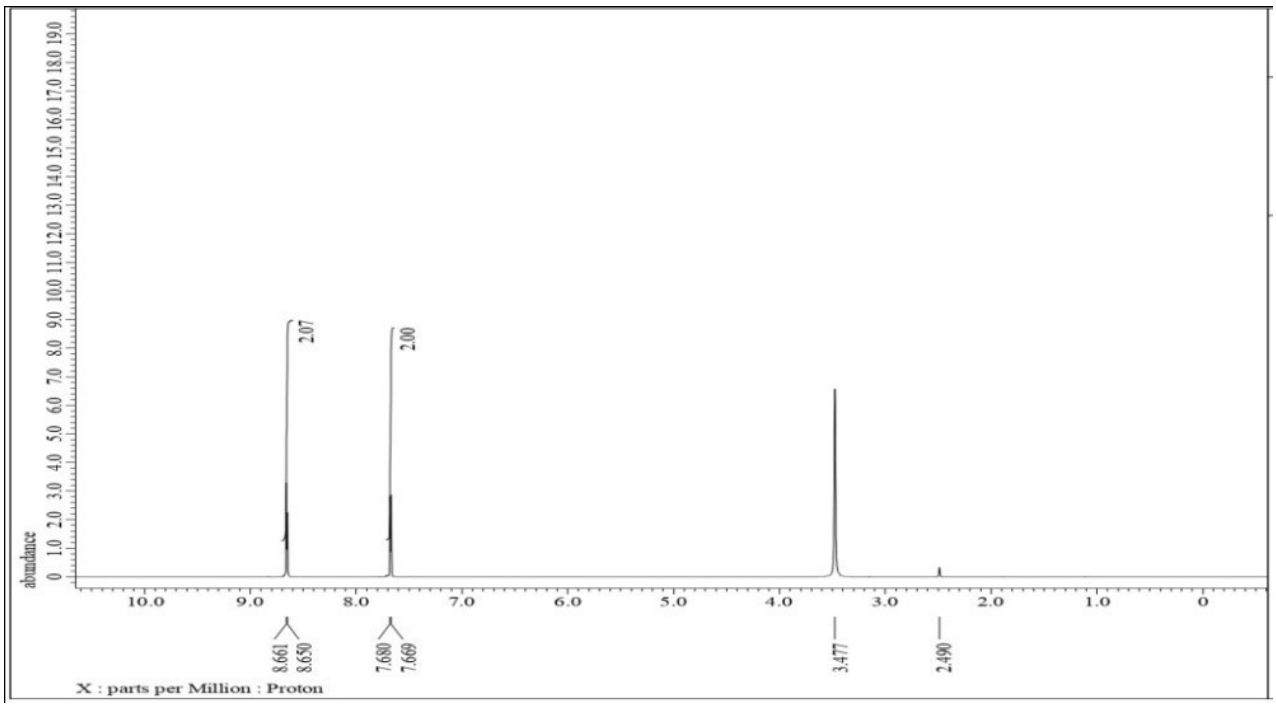

Supplementary Fig. 4. ^{1}H NMR spectrum of Kpot·H_2O

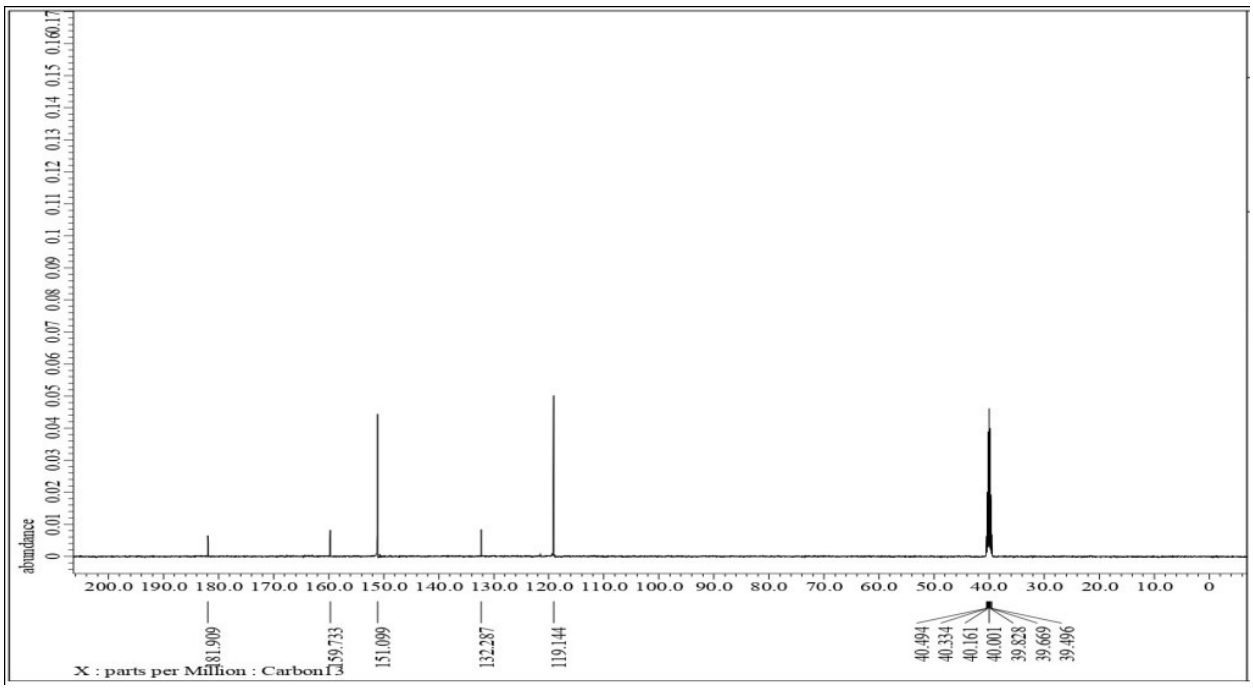

Supplementary Fig. 5. ^{13}C NMR spectrum of Kpot·H_2O

4. Electronic spectrum figure

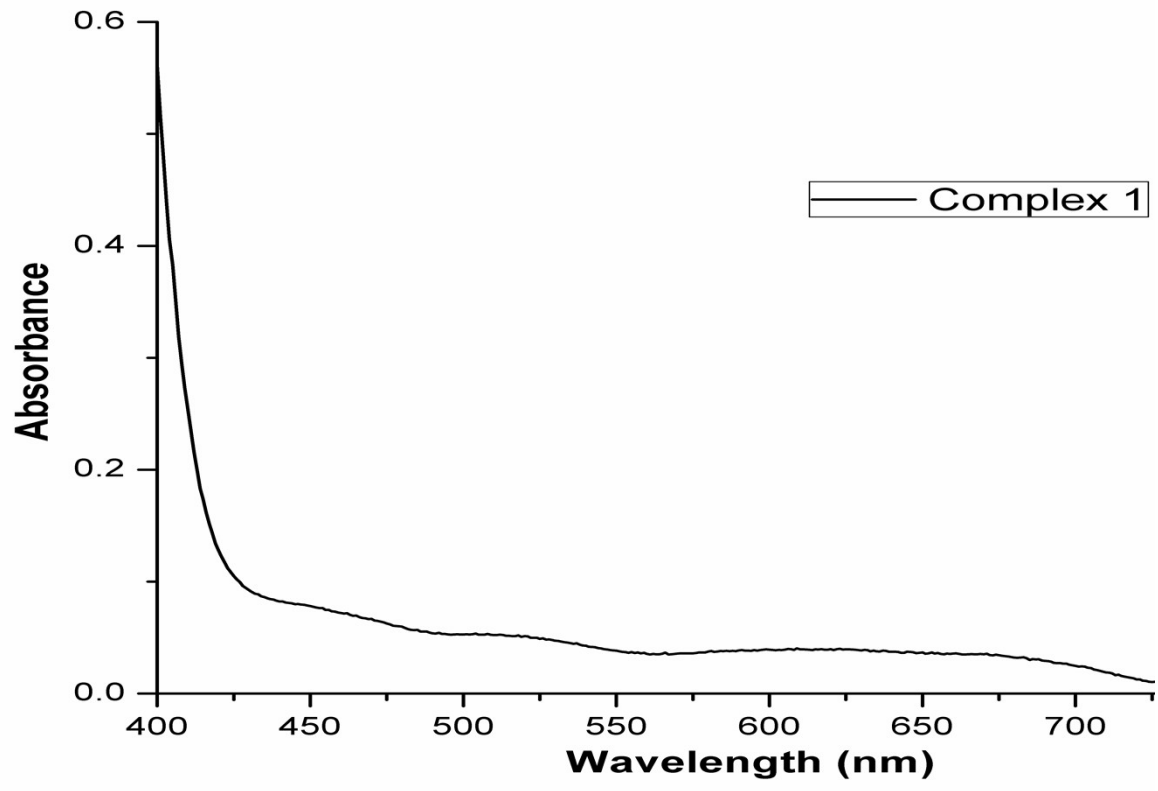

Supplementary Fig. 6. d-d Transition spectra of complexes **1** at 10^{-3} M in MeOH

5. Crystallographic Appendix

5.1 X-ray crystallography

X-Ray diffraction measurements of Kpot·H_2O and complex **1** were performed using Oxford Gemini and Bruker three-circle diffractometer equipped with a CrysAlisPro/CrysAlis CCD software using a graphite mono-chromated Mo Kα (λ= 0.71073 Å) radiation source at 296 K. The details of the temperature and monochromator of diffractometers are mentioned in the crystallographic data tables. Multi-scan absorption correction was applied to the X-ray data collection for all the compounds. The structures were solved by direct methods (SHELXS-08) and refined against all data by full matrix least-square on F^2 using anisotropic displacement parameters for all non-hydrogen atoms. All hydrogen atoms were included in the refinement at geometrically ideal position and refined with a riding model [7]. The MERCURY package and ORTEP-3 for Windows program were used for generating structures [8, 9]. Single crystals of complex **2** was was kept at 100.00 K during data collection. The material was recrystallised from methanol by slow evaporation. A suitable crystal was selected and the crystal was

mounted on a glass fibre oil on a Bruker APEX-II CCD diffractometer. Using Olex2 [10] package, the structure was solved with the SHELXT [11] structure solution program using Intrinsic Phasing and refined with the olex2.refine [12] refinement package using Levenberg-Marquardt minimisation and we have anisotropically refined the hydrogen atoms attached with the complex using NoSpherA2 [12] implemented in OLEX 2.

Supplementary Table 1. Crystallographic data for Kpot·H_2O, complexes **1** and **2**

Parameters	Kpot·H_2O	**1**	**2**
Empirical formula	$C_7H_6KN_3O_2S$	$C_{18}H_{24}CuN_{10}O_2S_2$	$C_{19}H_{29}BrN_{10}O_3S_2Zn$
Formula weight	235.31	540.13	654.94
Crystal system	Triclinic	Monoclinic	triclinic
Space group	P 1	P 21/n	P -1
T (K)	100(2)	566(2)	100(2)
λ, Mo Kα (Å)	0.71073	0.71073	0.71073
a (Å)	4.2204(14)	10.9088(14)	8.1195(4)
b (Å)	6.0284(19)	10.2087(9)	8.5613(4)
c (Å)	9.659(3)	11.9734(14)	9.9222(4)
α (º)	84.14(3)	90	97.183(2)
β (º)	80.32(3)	114.208(5)	109.571(2)
γ(º)	78.44(3)	90	99.479(2)
V, ($Å^3$)	236.73(14)	1216.2(2)	628.84(5)
Z	1	2	1
ρ_{calcd} (g/cm^3)	1.651	1.475	1.729
μ (mm^{-1})	0.756	1.106	2.776
F(000)	120	558	334
Crystal size (mm)	0.19 x 0.16 x 0.12	0.19 x 0.15 x 0.17	0.24 x 0.17 x 0.11
θ range for data collections(º)	3.458 to 28.987	3.287 to 25.347	2.221 to 26.372
Index ranges	-5<=h<=5, -7<=k<=7, -12<=l<=12	-13<=h<=13, -12<=k<=12, -14<=l<=14	-10<=h<=10, -10<=k<=10, -10<=l<=12
No. of reflections collected	1676	10634	6871
No. of independent reflections(R_{int})	1389	2208	2554
No. of data/restrains/parameters	1389 / 3 / 135	2208 / 0 / 151	2554/ 12/177
Goodness-of-fit on F^2	1.065	1.075	1.066
$R_1{}^a$, $wR_2{}^b$ [(I>2σ(I)]	0.0283, 0.0726	0.0391, 0.1098	0.0340, 0.0843

R_1[a], wR_2[b] (all data)	0.0300, 0.0759	0.0429, 0.1170	0.0393, 0.0880
Largest difference in peak /hole (e.Å^{-3})	0.223 and -0.278	0.613 and -0.393	0.726 and -0.882

[a]$R_1 = \Sigma||F_o| - |Fc||\Sigma|F_o|.$, [b]$R_2 = [\Sigma w\,(|F^2_o| - |F^2_c|)^2/\Sigma w|F^2_o|^2]^{1/2}$

Supplementary Table 2 Bond length (Å) and angles (°) for Kpot·H_2O

Bond length (Å)		**Bond angle (°)**	
K-S(1)#3	3.3303(16)	S(1)-K-K#1	74.25(3)
K-S(1)	3.4542(16)	S(1)#4-K-S(1)#3	78.01(4)
K-S(1)#4	3.3752(15)	O(1)#4-K-K(2)#2	79.00(5)
K-O(1)#3	3.037(3)	O(1)#4-K-S(1)#3	66.24(6)
K-O(1W)	2.691(4)	O(1W)-K-S(1)	80.01(10)
K-O(1W)#1	3.186(5)	O(1W)#1-K-S(1)#3	70.57(8)
K-N(1)	2.939(3)	O(1W)-K-N(1)#2	72.6(11)
K-N(1)#2	3.005(4)	N(1)-K-K#1	45.39(7)
S(1)-C(1)	1.702(4)	N(1)-K-S(1)#3	89.33(7)
O(1)-C(1)	1.383(4)	N(1)-K-S(1)	49.55(7)
O(1)-C(2)	1.357(4)	N(1)#2-K-O(1)#4	86.28(8)
N(1)-N(2)	1.404(4)	N(1)-K-N(1)#2	90.47(10)
N(1)-C(1)	1.304(5)	C(1)-S(1)-K	76.19(12)
N(2)-C(2)	1.291(5)	C(1)-O(1)-K#5	99.78(18)
N(3)-C(5)	1.340(6)	N(2)-N(1)-K#1	90.2(2)
N(3)-C(6)	1.319(6)	C(1)-S(1)-K#6	121.81(13)

Symmetry transformations used to generate equivalent atoms:
[1]-1+X,+Y,+Z; [2]1+X,+Y,+Z; [3]+X,-1+Y,+Z; [4]1+X,-1+Y,+Z; [5]-1+X,1+Y,+Z; [6]+X,1+Y,+Z

Supplementary Table 3. Hydrogen bonds parameters for $Kpot \cdot H_2O$

D-H···A	d(D-H)	d(H···A)	d(D···A)	<(DHA)
O(1W)-H(1WA)-N(3)#1	0.83(7)	2.03(7)	2.855(5)	174(6)
O(1W)-H(1WB)-S(1)#2	0.79(6)	2.57(6)	3.308(4)	155(5)
C(5)-H(5)-S(1)#3	0.95	2.93	3.745(4)	144.4

Symmetry transformations used to generate equivalent atoms: [1]2+X,-1+Y,1+Z; [2]1+X,+Y,+Z; [3]-1+X,+Y,-1+Z

Supplementary Table 4. Bond length (Å) and angles (°) for $[Cu(en)_2](pot)_2$ (**1**)

Bond length (Å)		**Bond angle (º)**	
Cu(1)-N(4)#1	2.096(2)	N(4)#1-Cu(1)-N(3)	97.09(9)
Cu(1)-N(4)	2.096(2)	N(4)-Cu(1)-N(3)	82.91(9)
Cu(1)-N(3)	2.101(2)	N(4)#1-Cu(1)-N(1	90.32(8)
Cu(1)-N(3)#1	2.101(2)	N(4)-Cu(1)-N(1)	89.68(8)
Cu(1)-N(1)	2.114(2)	N(3)-Cu(1)-N(1)	90.34(8)
Cu(1)-N(1)#1	2.114(2)	N(3)#1-Cu(1)-N(1)	89.66(8)
S(1)-C(1)	1.675(3)	N(4)#1-Cu(1)-N(1)#1	89.68(8)
O(1)-C(2)	1.352(3)	N(4)-Cu(1)-N(1)#1	90.32(8)
O(1)-C(1)	1.387(3)	N(3)#1-Cu(1)-N(1)#1	90.34(8)
N(1)-C(1)	1.312(4)	C(2)-O(1)-C(1)	104.17(19)
N(1)-N(2)	1.402(3)	C(1)-N(1)-N(2)	108.6(2)
N(3)-C(8)	1.467(4)	N(2)-C(2)-O(1)	113.4(2)
N(2)-C(2)	1.276(3)	N(1)-C(1)-O(1)	108.4(2)

Symmetry transformations used to generate equivalent atoms: #1 -x+1,-y+1,-z

Supplementary Table 5. Hydrogen bonds parameters for $[Cu(en)_2](pot)_2$ (**1**)

D-H···A	d(D-H)	d(H···A)	d(D···A)	<(DHA)
N(3)-H(3A)···N(2)#1	0.89	2.62	3.194(3)	122.9
N(3)-H(3A)···N(5)#2	0.89	2.52	3.255(4)	140.2
N(3)-H(3B)···S(1)	0.89	2.66	3.415(2)	143.8
N(4)-H(4A)···N(2)	0.89	2.64	3.208(3)	122.6
N(4)-H(4B)···S(1)#1	0.89	2.76	3.505(2)	141.8

Symmetry transformations used to generate equivalent atoms: #1 -x+1,-y+1,-z #2 x,y,z+1

Supplementary Table 6. Bond length (Å) and angles (°) for $[Zn(en)_2(pot)_2HBr{\cdot}CH_3OH$ (**2**)

Bond length (Å)		**Bond angle (º)**	
Zn1-N2	1.938(2)	N2-Zn1-N5	89.35(10)
Zn1-N5	1.954(2)	N2-Zn1-N4	89.68(10)
Zn1-N4	1.958(2)	N5-Zn1-N4	85.83(10)
S1-C1	1.675(3)	N5-Zn1-N4#1	94.17(10)
O1-C2	1.358(3)	C2-O1-C1	104.9(2)
O1-C1	1.375(3)	N1-N2-Zn1	117.83(17)
N2-N1	1.384(3)	C1-N2-N1	109.3(2)
N2-C1	1.331(3)	C2-N1-N2	105.3(2)
N1-C2	1.291(4)	C9-N5-Zn1	109.38(18)
N4-C8	1.486(4)	O1-C1-S1	121.2(19)
C5-N3	1.322(5)	N3-C6-C7	123.7(3)
O2-C10	1.393(17)	N1-C2-O1	112.8(2)

Symmetry transformations used to generate equivalent atoms: #1 -x+1,-y+2,-z+1

Supplementary Table 7. Hydrogen bonds parameters for $[Zn(en)_2(pot)_2HBr{\cdot}CH_3OH$ (**2**)

Supplementary Table 7. Hydrogen bonds parameters for $[Zn(en)_2(Hpot)(pot)]Br{\cdot}CH_3OH$ (**2**)

D-H···A	d(D-H)	d(H···A)	d(D···A)	<(DHA)
N(5)-H(5A)...S(1)	0.75(5)	2.64(5)	3.305(4)	148(4)
N(5)-H(5B)...Br(01)#2	0.72(5)	2.76(5)	3.387(3)	147(4)
N(5)-H(5B)...N(1)#1	0.72(5)	2.53(4)	2.992(4)	124(4)

N(4)-H(4A)...S(1)#1	0.72(5)	2.64(5)	3.288(4)	151(4)
N(4)-H(4B)...N(1)	0.77(5)	2.43(4)	2.932(4)	124(4)
N(4)-H(4B)...N(3)#3	0.77(5)	2.49(5)	3.128(4)	142(4)
C(5)-H(5)...Br(01)#4	0.85(7)	3.10(6)	3.685(5)	127(4)
C(6)-H(6)...S(1)#5	0.84(5)	2.83(5)	3.662(5)	174(4)
C(9)-H(9B)...Br(01)#2	0.92(5)	3.05(5)	3.614(4)	121(3)
C(10^a)-H(10A^a)...Br(01)#6	0.98	2.44	3.373(14)	158.8
C(10^a)-H(10B^a)...S(1)#1	0.98	2.79	3.527(12)	132.1

Symmetry transformations used to generate equivalent atoms:

#1 -x+1,-y+2,-z+1 #2 x,y,z+1 #3 -x,-y+1,-z #4 x,y-1,z #5 x-1,y,z-1 #6 x-1,y,z

5. H-Bonding interaction Figures

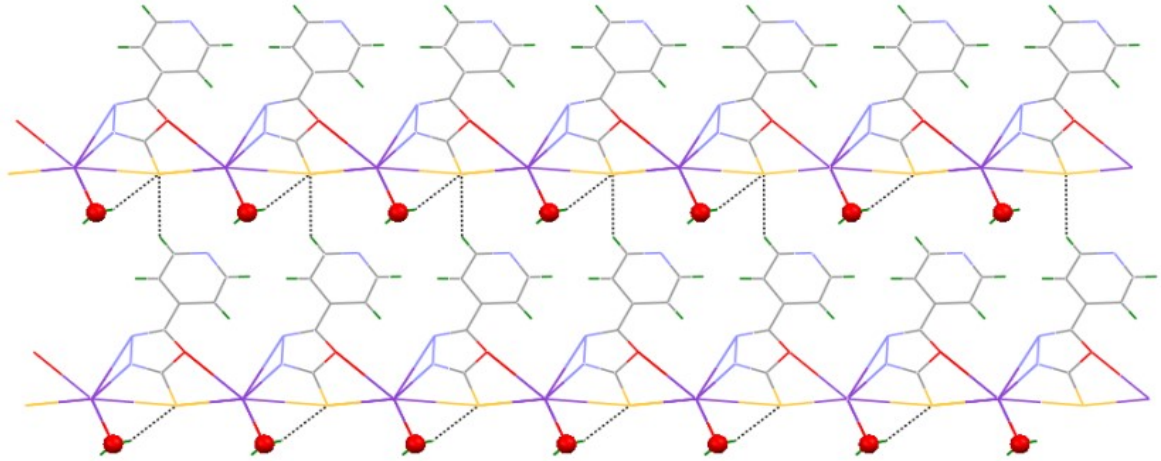

Supplementary Fig. 9 Showing O-H···S, C-H···S hydrogen bonding interactions leading to supramolecular architectures in Kpot·H_2O

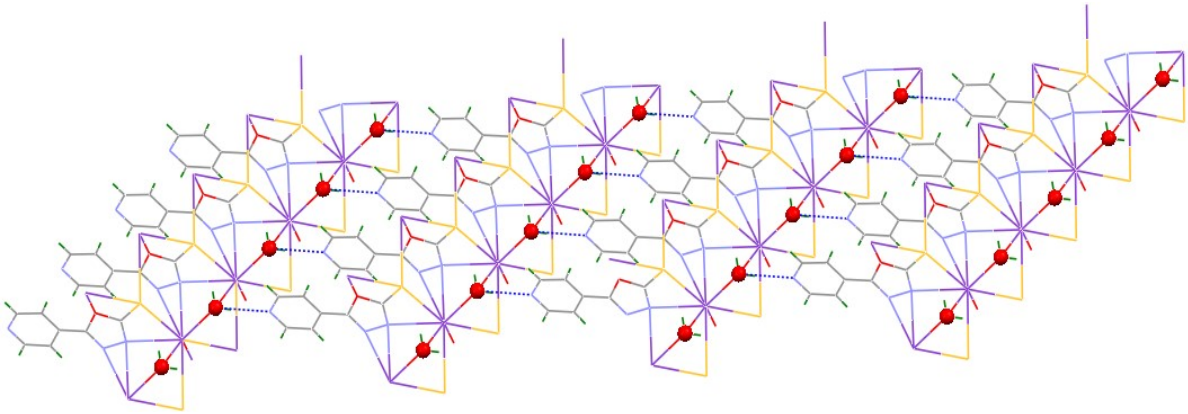

Supplementary Fig. 10 O-H···N hydrogen bonding interactions leading to ladder like structures in Kpot·H_2O

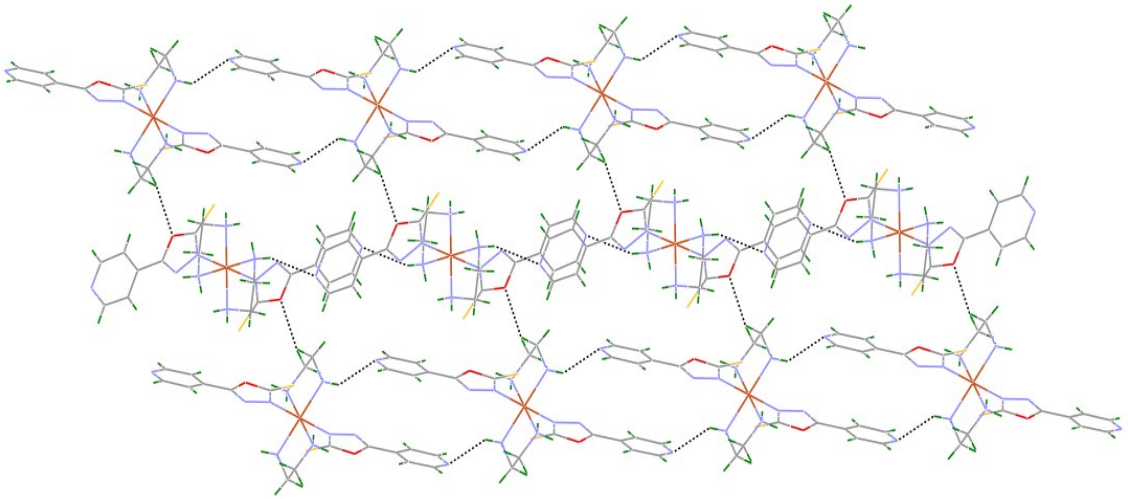

Supplementary Fig. 11 N-H···O and C-H···O hydrogen bonding interactions leading to a supramolecular structure in $[Cu(en)_2](pot)_2]$ (**1**)

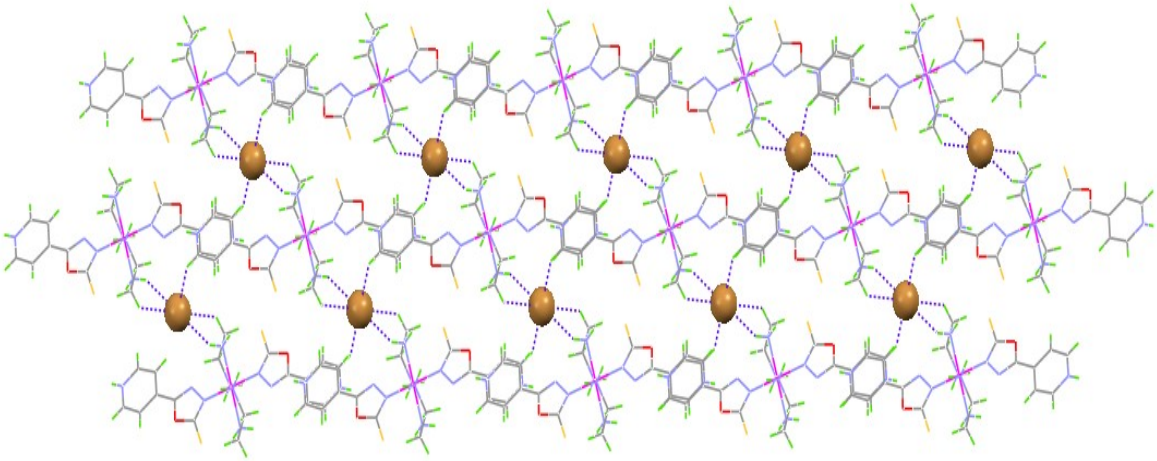

Supplementary Fig. 12. N-H···Br and C-H···Br hydrogen bonding interactions leading to a supramolecular structure in $[Zn(en)_2(pot)_2HBr{\cdot}CH_3OH$ (**2**)

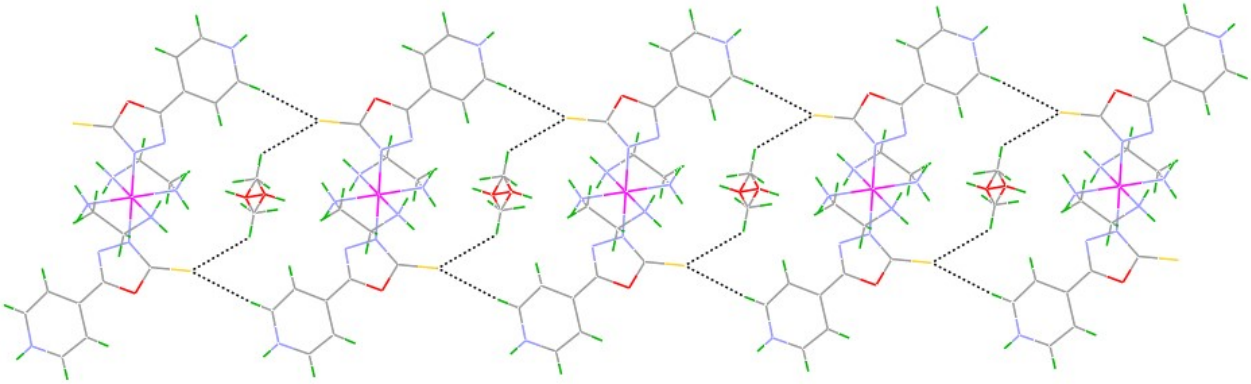

Supplementary Fig. 13. Showing C-H···S hydrogen bonding interactions leading to a linear structure in $[Zn(en)_2(pot)_2HBr{\cdot}CH_3OH$ (**2**)

Reference

[1] N. Rai, P. Gupta, A.Verma, R.K. Tiwari, P. Madhukar, S. C. Kamble, A. Kumar, R. Kumar, S.K.Singh, V. Gautam, *ACS Omega* 2023, **8**, 3768–3784.

[2] N. Rai, P.K. Keshri, P. Gupta, A. Verma, S.C. Kamble, S.K. Singh, V. Gautam, *Plos One,* 2022, **17**, p.e0264673.

[3] A. Verma, P. Gupta, N. Rai, R.K. Tiwari, A. Kumar, P. Salvi, S.C. Kamble, S.K. Singh, V. Gautam, *J. Fungi 2022*, **8**, 285.

[4] B.Y. Choi, H.Y. Kim, K.H. Lee, Y.H. Cho, G. Kong, *Cancer Lett.,* 1999, **147**, 85-93.

[5] P. Gupta, N. Rai, A.Verma, D.Saikia, S.P.Singh, R. Kumar, S.K.Singh, D. Kumar, V. Gautam, *ACS Omega* 2022, **7**, 46653–46673.

[6] N. Rai, P. Gupta, A. Verma, S.K. Singh, V. Gautam, *BioFactors,* 2023, 01-22.

[7] G.M. Sheldrick, *ActaCrystallogr. Section A*, 2008, **64**, 112-122.

[8] C.F. Macrae, I.J. Bruno, J.A. Chisholm, P.R. Edgington, P. McCabe, E. Pidcock, L. Rodriguez-Monge, R. Taylor, J.Van de Streek, P.A., Wood, *Appl. Cryst.,* 2008, **41**, 466-470.

[9] L.J. Farrugia, *J. Appl. Cryst*., 2012, **45**, 849-854.

[10] O.V. Dolomanov, L.J. Bourhis, R.J. Gildea, J.A.K. Howard, H. Puschmann, *J. Appl. Cryst.* 2009, **42**, 339-341.

[11] G.M. Sheldrick, *Acta Cryst.* 2015, **A71**, 3-8.

[12] L.J. Bourhis, O.V. Dolomanov, R.J. Gildea, J.A.K. Howard, H. Puschmann,. *Acta Cryst.* 2015, **A71**, 59-75.